

Investigation of the effect temperature on the performance of the photovoltaic solar design for the western Region of Paraná - Brazil

Cristobal Becerra-Díaz & Oswaldo Hideo Ando Junior

Federal University of Latin American Integration, Foz do Iguaçu, Brazil. eng.cristobal@gmail, oswaldo.junior@unila.edu.br

Received: October 23th, 2020. Received in revised form: April 24th, 2021. Accepted: April 28th, 2021.

Abstract

This paper show on impact of temperature decrease applied in Building Integrate Photovoltaics (BIPV) dimensioned on a photovoltaic solar tile with a superimposed photovoltaic arrangement model, in conditions of simulation of Standard Test Conditions for 1000 W/m² irradiation, for maximum and minimum summer temperatures of Foz do Iguaçu city during 2017-2018. The simulation (Comsol Multiphysics®) uses different types for material tiles (concrete, polypropylene and PVC) and compares the system considering the influence of the materials in the civil-structural characteristics of the roof. The results showed that the efficiency behavior with temperature variations, produce a decrease of linear efficiency. While the, tile designs proposal has a 16% efficiency value in the datasheet in the same conditions. The results shows a decrease of efficiency and power with the increase temperature in the same conditions of the study, obtaining the respectively value of 0.05%/°C and 0.24%/°C.

Keywords: building integrate photovoltaics; efficiency; solar tile; heat transfer.

Investigación del efecto de la temperatura en el rendimiento de un diseño solar fotovoltaico para la región oeste de Paraná - Brasil

Resumen

Este artículo muestra el impacto de la disminución de temperatura aplicada en Building Integrate Photovoltaics (BIPV) dimensionado sobre una teja solar fotovoltaica con un modelo de disposición fotovoltaica superpuesta, en condiciones de simulación de Condiciones de Prueba Estándar para irradiación de 1000 W/m², para temperaturas máximas y mínimas de verano de la ciudad de Foz do Iguaçu durante 2017-2018. La simulación (Comsol Multiphysics®) utiliza diferentes tipos de tejas de material (hormigón, polipropileno y PVC) y compara el sistema considerando la influencia de los materiales en las características civil-estructurales de la cubierta. Los resultados mostraron que el comportamiento de la eficiencia con variaciones de temperatura, produce una disminución de la eficiencia lineal. Mientras que la propuesta de diseños de baldosas tiene un valor de eficiencia del 16% en la hoja de datos en las mismas condiciones. Los resultados muestran una disminución de eficiencia y potencia con el aumento de temperatura en las mismas condiciones del estudio, obteniendo el valor respectivamente de 0.05%/°C y 0.24%/°C

Palabras clave: sistema fotovoltaico integrado en la construcción; teja solar; transferencia de calor.

1. Introduction

The growing concern for the diversification of the generating base and the constant search for energy sustainability has driven the search for new energy sources and the spread of unconventional renewable energy use [1], demanding the transition to a green economy with the implementation of specific public policies and regulations,

also imposing on the productive sector innovative actions of sustainability [2]. In this regard, Brazil has assumed a prominent role in the world stage due to its predominantly hydro generating base and the implementation of incentive programs, such as the “Incentive Program for Alternative Sources of Electricity”, which aims to encourage investment in new sustainable technologies [3]. However, despite the political and economic efforts in Brazil with the allocation of

How to cite: Becerra-Díaz, C. and Ando Junior, O.H., Investigation of the effect temperature on the performance of the photovoltaic solar design for the western region of Paraná - Brazil.. DYNA, 88(217), pp. 185-199, April - June, 2021.

R \$ 226 million for investment in mitigation projects, adaptation to climate change in 2011; and federal renewable energy incentive laws, the diversification of the generating base in relation to the GDP has been late when compared to the Latin American level with countries like Costa Rica and Uruguay [2,4,5].

Currently the Brazilian energy matrix is conditioned to the national hydraulic supply [6], showing a strong dependence on the rainfall, which added the constant climate changes between the years 2012-2017. Resulted in periods of irregular rainfall causing a reduction in the volume of the reservoir and consequently, the significant increase in energy prices by the use of thermal generation as back-up system [7,8].

Among the possibilities of diversification of the Brazilian generating base, alternative sources have emerged, such as wind and photovoltaic energy. It is evident that the wind potential is the second highest in the country, with values ranging from around 60,000 MW (depending on the methodology employed) [9]; together, among unconventional renewables, the cost of wind is one of the lowest due to the return on investment [10].

Regarding the photovoltaic solar potential in Brazil, it has such high values of direct irradiation that reached 2400 kWh/m².year in regions such as Bahia and Paraíba. In addition, it's possible to generate more solar electricity than in the sunniest place in Germany which possess large investments in generation with this technology [6]. It is important to highlight that in summer months; the generation is maximum in the extreme south and southeast states of Brazil and coincides with the maximum demand registered by ONS for these regions. In this context, photovoltaic solar generation also has a great potential to contribute to the reduction of the demand peaks of the SIN transmission systems [6,9].

Given the above, and considering the possibilities it presents in the national territory for the massification of alternative sources of energy, photovoltaic solar is promising for the use of alternative energies.

New PV generation techniques include building-integrated photovoltaic generation technologies, also called Building Integrate Photovoltaics (BIPVs), which adapt to the original design of the architectural project. These techniques replace the structure's cladding materials, saving on the total cost of installation. In addition, they contribute aesthetically to the building and provide unique features that can assist in thermal comfort depending on the constituent material. [11].

From the point of view of energy efficiency, BIPVs are "ideal", as power generation and consumption have coincidence, thereby minimizing transmission losses that occur in traditional power systems [12].

The BIPVs have a wide range of methodologies for the installation of photovoltaic systems, among which stand out facades, windows, walls, roofs and shingles for being better known. It is this last classification that presents the real interest of BIPVs in this research, since solar tiles with integrated solar tile are a new product, still in improvement and with ample possibility of improvement.

In Brazil, the residential and commercial sectors are responsible for 23% and 11% respectively of the total

national consumption of electricity, where ventilation and air conditioning equipment account for 50% of summer consumption, up to 70% in glazed buildings [12]. In this context, this article presents the analysis of the influence of operating temperature on the performance of a photovoltaic solar tile (TSF) for residential and land use of small incorporated into the construction (BIPVs) to the west of Paraná - Brazil.

Increasing photovoltaic cell temperature is a critical problem that impacts system performance, causing drastic yield reduction, material degradation and reduced lifetime [13]. As cell temperature increases, the mobility of electrons and holes in the material decreases, increasing the resistivity value of the photoconductor according to the mass action law. Moreover, while increasing the operating temperature, there is a drop in the open circuit voltage value, reducing the value of the power delivered to the load. [14].

This problem has been widely studied under various conditions for conventional modules, but the specificity of BIPVs has not been covered, especially TSFs. Given the above, this research aims to investigate the effects of operating temperature on the efficiency of cells incorporated into solar tiles, and verify the behavior and analyze other factors that affect the solar tile and directly to the structure.

For the PV evaluation purposes, the reference values at Standard Test Conditions (STC) were used for irradiation in 1000 W/m² and temperatures of 25°C [15]. However, such conditions rarely occur during daily operation, so it is important to evaluate the solar tiles front of actual operating conditions, with daily variations in ambient temperature and quantifying the influence of factors such as wind speeds, thermal properties of materials, TSF geometry and their influence on system behavior.

This paper present of study and verify the influence of temperature on the performance of the Solar Tile incorporated into the building for different technical arrangements (Material - Photovoltaic Solar Arrangement), considering heat transfer conditions with the environment by conduction mechanisms and the convection and radiation from data literature.

The main contribution of this research in modelling is a specific analysis of the performance of the proposed technical arrangement on the influence of operating temperature on the efficiency of cells incorporated in the solar tile, which aims to fill the existing gap on BIPVs studies. It is noteworthy that the importance of this research is to determine the operating temperature of the PV array at STC. Therefore, it is essential to propose studies and analysis of this issue. However, the effects of this problem have not yet been studied for TSF, which have distinct characteristics from conventional photovoltaic systems, as they interact directly with the building structure materials, which need analysis to verify their influence on operating conditions and yield from TSF.

While the contribution of this research to the proposed technical arrangement, the commercial model of flat tile and single crystalline silicon cell has been modified, with an approximate 16% efficiency for conventional cells, to an overlapping format cell, as this configuration has not been studied or commercially developed. Based on this product, it

is intended to verify the characteristics while differentiating the influence of thermal effects for different conditions.

Concerning the constituent materials, the research contribution incorporates materials that have not been used for the construction of BIPVs on tiles, reason why the innovation of materials is planted, using concrete, Polypropylene and Polyvinyl Chloride (PVC). These materials were considered to characterize and contribute in the cell as a function of the influence of heat transfer as well as structure as a function of material weight, mechanical strength and thermal comfort.

The Section 2 showed the photovoltaic technologies and arrangements, describing the field of action, the materials that make up the panels and their respective efficiencies. BIPVs will be discussed in more detail, characterizing their uses and aspects for implementation and a brief comparison between the different factors of PV and BIPVs. In addition, the state of the art of BIPVs technologies, current regulations and regulations will be addressed. The Section 3 presents the dimensioning and modeling of the chosen models of photovoltaic solar tile (low cost), the geometry of the studied solar tile, detailing the materials and constituents of the evaluated photovoltaic arrangement. The Section 4 shows the correlation of the results and the comparison of the proposed models with the materials, the cell temperatures and the determined efficiencies. Finally, in Section 5 there are the conclusions of this article on the design of the solar tile and the use of Building Integrated Photovoltaics (BIPVs) technologies.

2. Building Integrate Photovoltaics (BIPV)

The photovoltaic technologies can be classified in several ways, one of them is by grouping the range of existing technologies into current and possible future options, classifying them into 1st, 2nd and 3rd generation [16].

The current production of PV technology, corresponding to the 1st generation, is dominated by single-junction cells based on monocrystalline silicon wafers (m-Si) and polycrystalline silicon (p-Si), with laboratory efficiencies ranging from 18% to 21% but high cost [17]. However, the m-Si commercial model is manufactured with efficiencies between 13-14% for a lower market value [18]. Half the cost of 1st generation PV is 200-250 microns thick silicon junction, a superlative cost, as most solar absorption occurs in the first 10 microns. Therefore, reducing “wafer” thickness offers potential cost savings [16,17]. Despite much scientific progress, 1st Generation PV costs an average of US \$4/W, which is still about 4 times more expensive for truly competitive commercial production [18].

The 2nd generation of the PV is a reduction of US \$/W, reducing the material, by using thin film devices, while maintaining the efficiencies of the 1st generation [17]. Use Amorphous Silicon (a-Si), a thin film Copper-Indium-Selenium (CIS) association, Cadmium Telluride (CdTe) or Polycrystalline Silicon (p-Si) deposited on low cost substrates such as glass [16]. Cost savings have been made possible by the fact that CdTe, CIS and a-Si technologies absorb the solar spectrum much more efficiently than m-Si or p-Si, using between 1-10 μ m active material [17].

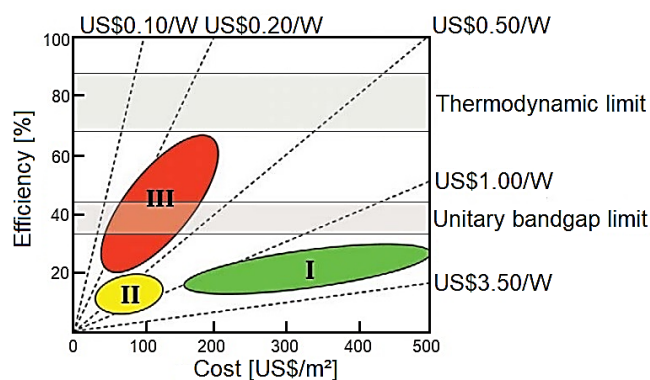


Figure 1. Cost comparison, efficiency for three generations of solar cell technology: single junction, thin film and advanced film. Source: Conibeer, 2007.

Recent laboratory scale research shows the potential of thin film, with efficiencies of 16.5% CdTe and 18.4% CIGS [19], however, CdTe and CIGS PVs have been slow to scale commercially. This is partly due to the gap between laboratory efficiencies and commercial production module efficiencies of 10.7% for CdTe [19] and 13.4% for CIGS [20] which are low as a result of unresolved issues related to material reproducibility and uniformity over large areas [17]. Given the precursor progress of thin film silicon over the last few years, the trend indicates that the potential of 2nd generation is more likely to be realized by silicon based thin film devices, enhanced by the development of production tools for the flat tiles industry [17].

3rd generation deals with devices that may or may not exceed single-junction limits and feature ultra-high efficiency for the same production costs as 1st and 2nd generation, improving m-Si and p-Si efficiency and reducing cost from US\$/W [16]. This technology uses thin films applied to low cost substrates to maintain material economy and increase efficiency.

In addition to using thin and triple junction films, this technology includes organic materials (OPV) and quantum dot products (PQs), with both technologies still under development [19]. Although 3rd generation PV still lacks conversion efficiency, they exhibit great potential and several advantages over established technologies, including low cost processing over large areas, study of semi-transparency effects, mechanical flexibility and low weight [19]. Applications of these devices include low power equipment (for residential use) and building integration known as Building Integrated Photovoltaics. The comparison of the three PV generations in terms of efficiency, cost of US\$/W and US\$/m² is shown in Fig. 1.

As shown in Fig. 1, 1st and 2nd PV technologies do not reach 30% efficiency for the unit bandgap limit, while 3rd generation PV technologies are close to reaching the thermodynamic limit, with efficiencies close to 70%. Costs of US\$/m² from 1st to 2nd generation decreased by 350 US\$/m², so the transition from 2nd to 3rd generation had a slight increase from 150 US \$/m² to 200 US\$/m², which can be explained by the huge increase in efficiency from one technology to another. Regarding US\$/W costs, 3rd generation has the most cost-effective technologies ranging

from US\$0.15/W to US\$0.30/W, considerably reducing US\$3.5/W to US\$1.00/W 1st and 2nd generation PV. Therefore, the current tendency is to improve the costs of US\$m2, US\$1.00/W and the efficiency of the 3rd generation.

2.1 Photovoltaic systems incorporated in construction

The BIPVs address the solar photovoltaic technologies that can be installed on the surface of the building structure, allowing the possibility of combining the transformation of electricity with additional functions such as: building material coverage, weather protection, thermal insulation, acoustic protection, thermal comfort, shading, etc. [21,22];thus transformed the energy consumer building into an energy producer [23]. BIPVs become true building elements, installing on any exterior surface of the building, offering applications for roofs, walls, facades or windows, among others [24]. BIPVs can be characterized according to their opaque or semi-transparent properties and depending on their applications. A representative scheme of this division can be seen in Fig. 2.

Installation of BIPVs products is constantly growing as an innovative technology, so manufacturers continue to create new products and designs to meet market demands. [23]. Similarly, the implementation of feed-in tariffs and the interest in setting specific targets for zero net energy buildings (NZEBS) [25] and other government incentives for solar power have caused widespread acceptance worldwide [26].

Global development of BIPVs technology reached approximately 2000 MW of installation by the end of 2016 [27], western Europe being the largest market BIPVs products and recently had a growth in Eastern Europe [28]. With respect to current market applications of BIPVs, they reach about 80% for assembling roofs and the remaining 20% in facades and other components [23].

These products rely on the power grid as a back-up system when demand exceeds generation, without the need for oversizing of the system, as occurs in isolated systems that must take into account the worst case of solar supply and seasonality in most of the regions [12].

Due to the concept of synchronization, in which generation and consumption occur simultaneously, the BIPVs assist the electric utility distribution system (load relief), which results in energy savings and increased service life of the distribution system equipment [12].

For BIPVs systems to be multifunctional in structure, whether in tile, wall, facade or window format; there are

several factors that should be considered, including: (i) Operating Temperature of Cell and/or Module; (ii) Maintenance, Shading and Solar Orientation and (iii) Irradiance. Among these factors, the irradiance and temperature of the module should be considered as the most relevant factors, as they affect both the electrical efficiency of the system and the energy performance of buildings where BIPVs are installed [29,30].

It is important to highlight that both the economic and environmental benefits of applying solar PV to the built environment are not fully established, as it is a new and poorly studied technology. Thus, there is a need to demonstrate that the integration of integrated photovoltaic solar installations into the building is much more than just a good idea, but it also brings great benefits to the user, the electrical system and society.

2.2 Comparison of conventional photovoltaic systems and built-in photovoltaic systems

Factors to be considered for performance comparison between conventional PV and BIPVs include: (i) efficiency; (ii) inversion cost; (iii) economic profitability; (iv) reliability; (v) avoided busts, among others. These factors will directly influence the choice of one technology or another for a particular application in a given location depending on the characteristics of the region and the location to be installed. Table I shows a comparative table between conventional PV and BIPVs.

As shown in the comparison of Table 1, BIPVs offer better cost-effectiveness over centralized photovoltaic systems by avoiding the cost of land acquisition or use of ground area for supporting structures, as well as avoiding necessary cabling costs. for a PV system installed at a remote location [31].

Table 1. Comparison between conventional PV and BIPV products.

Conventional PV connected to the network	BIPV
Widely known and used technology	New and still developing technology.
Abundant market supply, technology present worldwide.	Market for North America and Western Europe, lowest offer for Eastern Europe and Asia.
Easy to install, no additional roof support required.	Difficulty of installation. Depending on the type of BIPVs, requires replacement or replacement of structure.
Low production cost due to the massification of technology.	High cost of production, few producers.
Low acquisition cost for large amount in the market.	High acquisition cost, few suppliers and is restricted to a higher economy class.
Slightly higher efficiency because it is a proven technology.	Slightly lower efficiency, new and developing technology.
Limited to roof top or ground mounted.	Wide application. Employed on roof, wall and/or window, among others.
Widely developed and well-known mounting standard, requires no differentiated technical knowledge.	Limited assembly knowledge requires differentiated technical training.
Requires installation of T&D system.	It does not require complex T&D systems.

Source: Adapted from Shukla et al., 2017; Shukla et al., 2016; Shukla et al., 2015 and Biyik et al., 2017.

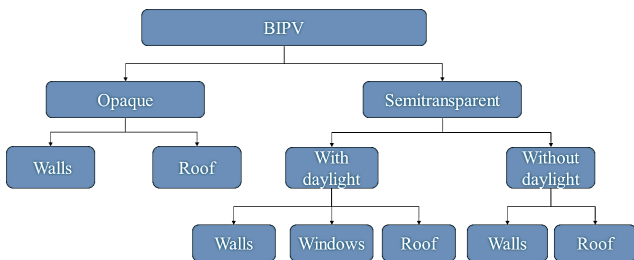


Figure 2. Characterization of BIPVs
Source: Debbarma, et al., 2016.

In addition, solar buildings produce electricity at or near the point of use, avoiding T&D costs and associated losses, such as in commercial installations where electricity demand (9am to 17pm) usually coincides with the peak of the electricity supply [35].

As well as in BIPVs in regions that are plagued by waves and heat in the summer, there are spikes in demand due to excessive use of air conditioning devices, which may result in a decrease in the cost of building electricity bills and a decrease in ampacity. In other words, the maximum current load that a device can carry is reduced, avoiding overloading of the system due to the equipment overload [36].

2.3 State of the art

The complex thermal interactions that occur when exchanging heat between a photovoltaic system and the building in which it is integrated has been the subject of numerous investigations in recent years, motivated by the problem of increasing the energy of photons exceeding the bandgap or more simply called increasing cell temperature, limiting its efficiency mainly due to the increase of internal resistance, generating energy losses [20,37,38].

Among the most cited heat transfer studies in solar facade-type BIPVs, a simplified method for calculating the cooling loads that reach the internal environment through the building walls is proposed. Comparing brick facades with and without integrated PV systems, the study demonstrates that the reduction in cooling load consumed primarily by air conditioning equipment is approximately 42%, as the outer air layer removes the heat absorbed by the PV surface. closest to the PV system [39].

Meanwhile, M. Sandebergh conducted a study based on simulation and experimental analysis of prototypes to characterize the heat transfer of solar facades, but with air ducts; aiming to analyse the performance of a hybrid facade that in addition to generating electric energy would take advantage of thermal energy, using heat dissipation from photovoltaic modules as environmental heater on cold days. In the study, it was concluded that 40% of the heat that hits the surface of the solar facade is transferred to the surface of the facade by radiation, working the channel as an isolated surface and with opening regimens, resulting in an optimal behaviour for the heat sink functions. heat and indoor environmental heating [40].

On the other hand, Krauter experimented with solar facade configurations in Rio de Janeiro, comparing ventilation types, using mineral wool and a hybrid with water as insulation. The study proved that the production of electric energy results in an increase of between 8% and 9,3% in the studies performed [41]. Despite the performance improvement, the study highlighted the high cost that makes the proposal economically unfeasible.

Gutschker O. & Rogass H. continued Krauter's research by simulating and characterizing a hybrid facade with the same purpose using numerical methods. The results obtained are similar to Krauter, with maximum air duct temperatures between 45°C and 50°C for outdoor air temperature of 25°C concluding that the amount of heat transmitted by the ducts is proportional to the increase of the outside temperature [42].

As early as 2004, Yang monitored the first building in Hong Kong to have an integrated PV system, where 8 kWp of 250m² was distributed between decks and facades, to 100 mm thick concrete walls [45]. In the study, it was shown that the impact of ventilation in the air chambers is negligible for the vertical parameters at this latitude in the modules, but is highly efficient for decreasing the annual ventilation load.

In Spain, one of the first PV facades was held at the Pompeu Fabra Library in Mataró. In this structure, the temperature problem was treated in terms of thermal transmittance to calculate the energy transferred inside the Building [43]. The library was considered not to have good thermal integration between the building materials and heat dissipated by the modules, but because of natural ventilation, the modules reach maximum temperatures of 45 °C even in summer months [44].

Based on accumulated project experience PV-Hybrid-PAS and IMPACT, the Joint Research Center of Ispra from Itália, developed an outdoor experimental cell called TRE (Test Reference Environment), which sought to establish European standards of evidence for BIPV modules for forced ventilation system [38]. Based on this cell, in 2012 Lodi et al developed an improved version of the cell with the objective of using the module's residual heat for air conditioning, avoiding overheating and, consequently, reducing efficiency [45]. Test results have shown that the use of 115 mm inner tubes, with forced velocity of 0.23m/s to 1.91m/s has favorable results for dual-function ventilation and air conditioning, but the study should be adapted for large-scale commercial and low-power residential use.

Through parametric study of different types of high-efficiency glass, Ng & Mithraratne researched the integration of thin-layer cells in building windows in Singapore (tropical climate) [46]. The results revealed that among the effects through the parametric study of different types of high-efficiency glass, Ng & Mithraratne investigated the integration of thin-layer cells in the most significant building windows in Singapore (tropical climate) that influence the efficiency and PV window power generation is shading and frame material. Shading cannot be modified, only predicted; but the correct material of the structure is fundamental for reducing the thermal effect without the use of cooling, which in most cases lowers the temperature but is a power consuming [47].

A different approach to mitigating temperature rise in cells without the use of refrigeration systems is the use of Phase Change Materials - PCM, materials that store latent heat energy and allows to choose the phase shift point [48]. Huang et al studied the thermal variation of these materials under different irradiance conditions in order to verify the temperature behavior. The results showed that with irradiation intensity of 750W/m² the outside surface temperature of the structure varies by less than 1°C and is a perfect absorber to be used as a complement to PV structures.

Ma et al, perform a PCM review to regulate efficiency in PV structures. Among the methods covered by the study, a practical solution to decrease the temperature effect is to increase the typically low thermal conductivity properties of PCM [49]. In addition, the insertion of metalline fins in the materials significantly improves the PCM characteristics,

making the temperature distribution and therefore the heat dissipation in the module more uniform [50]. However, based on the review of the revised literature, the simple PV-PCM system may not be economically viable if used only to improve PV conversion efficiency, because PCM alone does not represent a holistic solution to the temperature-efficiency problem in PV structures.

In Brazil, the first proposal for a grid-connected BIPVs system was put into operation on the campus of the Federal University of Santa Catarina (Florianópolis) in 1997 [51], with a system designed to meet the typical urban demand of four people on an annual 2078 Wp [12]. Subsequent to this first venture, several BIPVs were installed within the context of “testing systems”, in order to verify their behavior, thus a large percentage is installed in colleges and research centers such as: 1,15 kWp on UFSC in 2000 [12]. A 6.3 kWp system installed at the University of São Paulo (IEE/USP) in 2001, a 10 kWp installation in 2003 at UFSC [52], and a 44.4kWp flexible module system installed in the front building of the Petrobras Research Centre in 2003 [12].

Due to the BIPVs installed in the 2000s, the integrated solar market and its use has been widening, becoming incorporated into the structure in large buildings, such as the solar system incorporated in the roof of the Governador Magalhães Pinto stadium, in Belo Horizonte, in 2014; becoming the first large-scale BIPVs system [53]. This initiative was replicated within the context of the 2014 World Cup, and PV roofing systems were installed in several sports centers, being the pioneers in large-scale BIPVs in Brazil (Maracanã - 400 kWp, Mané Garrincha - 2500 kWp, Pitucaçu - 400 kWp) [54], [55].

At the same time, BIPVs were incorporated into important industrial projects, especially the partnership of Organic Photovoltaics Cells - OPV developed by CSEM Brazil, the only Brazilian company that can supply organic photovoltaic modules and adapt them to BIPVs through metal tiles manufactured by Medabil company, products that are used in the construction of large warehouses [56].

However, the inclusion of solar structures in both industrial and large-scale installations has been developed by foreign technology, so it should be noted that scarce national production. This has negatively affected the installation of low voltage residential and BIPVs, as it remains a high cost technology and few suppliers. The fact that the limited producers of BIPVs in Brazil is evidenced in the search in the patent office of the National Institute of Industrial Property, as it has few specific projects for solar buildings, besides using 2nd generation silicon plates. Latest patents include ECO Solar Roof, which began operating in 2018 for solar roof production [57].

With regard to the world market, North America and Western Europe dominate in both the development of BIPV-specific technology and the number of companies offering this service. In the field of solar tiles or roofs, the market is dominated by Tesla Company, which has the largest technological development in unitary tiles adapted to the structure for residential and low voltage applications. The product is based on the Panasonic Model N3300 HIT solar panel, with a standard electrical efficiency of 19.7% for conventional PV modules, but has a reduction of up to 16%

when installed on photovoltaic solar tiles, depending on the efficiency losses of this technology [58].

2.4 Standards, regulations and certifications

The normative legislation and regulation governing the production, transmission and distribution of electricity in Brazil does not yet consider as a specific case photovoltaic solar systems integrated with urban buildings and interconnected with the conventional electricity grid. Even the technical-political-normative insertion of this technology is still a topic of debate around the world [12].

The National Electric Energy Agency (ANEEL), fits BIPVs systems into grid-connected photovoltaic systems (SFCR) for power below 10kW, being governed by the same decrees, laws and regulations. In this sense, photovoltaic systems integrated with urban buildings that are connected to the public grid can be characterized as self-generators of electricity (APs).

Even with the little progress made by Brazil in the introduction of PV microgeneration, where investments are mostly financed by the owners with very high rates and fees, resulting in a long payback period, which consequently slow down local microgeneration and market expansion, there are already some tax breaks for certain photovoltaic equipment [59].

Comparing Brazil's financial incentive with US market incentive policies, these provide national and state incentives for PV installation (including BIPVs) approximately 30% of the value of the venture and with very low interest. This result in a high growth rate of PV, which in turn has led to an increase in the market, falling technology prices and further development of PV and its ramifications.

3. Design of the solar tile

This section presents the design of the solar tile showed the hypotheses adopted for conduction heat transfer and the convection and flow data from the literature. The base geometry of the chosen tile is of flat shape with incorporation of superficial PV arrangement.

This format is one of the most common in the market and is easy to replace if material fails or ruptures. It is also easier to build than curved roof tiles, has good roofing and is easily adapted to photovoltaic cells [60-66]. From the standard rectangular flat tile format, two models have been proposed which are: Model 1 - Tile with Overlaid Photovoltaic Arrangement and Model 2 (tile with integrated photovoltaic arrangement). The integrated and overlapping models are shown in Fig. 3 (a) and Fig. 3 (b) respectively.

Model 1 is intended to be a different product to the market with a spare photovoltaic tile geometry. This model aims to determine if the overlap of the PV array over the tile has distinctive features to the commercial model (integrated system), because the effects of heat transfer between the tile and the PV arrangement happen differently with less contact area.

On the other hand, in order to determine the characteristics of the standard and commercial model for the proposed TSF materials in Model 2, the insertion of the PV arrangement in the tile is evaluated. By having a larger contact area between the surfaces, the heat transfer effects

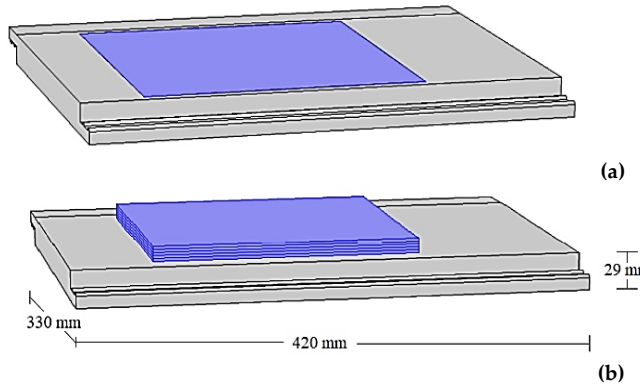


Figure 3. Modeling of the tile with the photovoltaic arrangement: (a) Integrated model; (b) Overlay Template
Source: The authors.

happen differently, so they reach different temperatures to the overlapping model, which consequently affect the PV arrangement. When modelling and implementing both models in the 3D structural simulation environment in Comsol Multiphysics® software one has that the overlay or insertion of the photovoltaic array in blue color, as shown in Fig. 3.a) for the integrated model and Fig. 3.b) for the overlay model.

For the photovoltaic cell modelling, the same materials and dimensions were kept in both models. It should be noted that the main difference between the two models is in how the temperature will influence the tile and the turn in the photovoltaic cell, as the surface of the integrated model experiences conduction heat transfer influenced by all PV array components and the tile. Whereas in the superimposed model, the heat exchange by conduction takes place only by the last layer of the PV (EIVax) arrangement with the tile, until it reaches the photovoltaic cell arrangement.

By analyzing Fig. 4 it can be seen that the photovoltaic cell was approximated by the geometry of five coupled

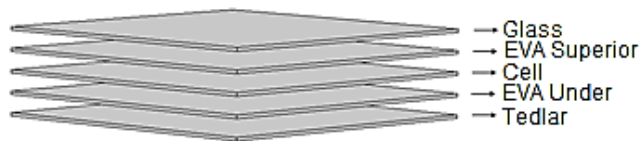


Figure 4. Photovoltaic system composition
Source: Adapted from Leow *et al.*, 2016.

Table 2.
Thermal properties component tile and module.

Nº	Material	k[W/m °C]	Cp[J/Kg °C]	ρ[kg/m³]
1	Glass	1,80	500	3000
2	EVA superior	0,35	2090	960
3	Cell	148	677	2330
4	EVA under	0,35	2090	960
5	Tedlar	0,20	1250	1200
6	Concrete	1,80	880	2300
7	PVC	0,10	850	1760
8	Polypropylene	0,25	1700	910

Source: Adapted from Leow *et al.*, 2016; BRASKEM, 2012 and IMCPLAS, 2018.

plates, with 220 mm of square surface and 2.5 mm of thickness each, totaling 12.5 mm system thickness. The PV array was designed according to the typical components of a photovoltaic system composed of a layer of glass, Ethylene Vinyl Acetate (EVA) and a layer of Vinyl Polifloururo (Tedlar). The thermal properties used in the simulation of the PV array (Nº. 1 to Nº. 5) and tile (Nº. 6 to Nº. 8) array components are listed in Table 2.

A number of literature and studies were revised, such as: Radziemska on the effect of temperature on crystalline silicon cells [13]; Barring the influence of temperature on photovoltaic solar cells [14]; Omer et al on poor PV cell performance in monitoring a BIPV system in the UK [60]; Agrawal & Tiwari in Energy Analysis and Exergy in a BIPV System [61], Portolan & Rüter characterizing the potential of BIPV and Building Applied Photovoltaics (BAPV) in a Brazilian home, demonstrating that temperature affects cell power [65], Essah et al in Performance Evaluation of a BP m-Si Integrated PV System [64]. Those authors demonstrated that temperature has a strong influence on module/cell efficiency and consequently on system power.

In order to analyses the technical arrangement operating under average conditions, it was decided to perform the tests for the average minimum and maximum summer temperatures of Foz do Iguacu from 21/12/2017 to 20/03/2018. According to data from the National Institute of Meteorology (INMET), the average maximum and minimum temperatures measured for the summer months was 30,6 °C and 22,1 °C which corresponds to the hours of 17h and 6h respectively [71].

It is important to highlight that the territory under analysis presents extreme temperatures of maximum and minimum divergent to the average. In the sample universe, the average values of maximum and minimum temperatures represent 71% of the annual samples [71], the remaining 29% corresponds to extreme sample values that occur in isolated cases of maximum or minimum temperatures.

3.1 Scaling by analytical method

The tests were performed on the STC (Standard Test Conditions) of irradiation of 1000 W/m², for a single tile model, considering the simulated heat conduction effects in Comsol Multiphysics® software, and the convection and radiation specified with literature data. For greater accuracy of results, the mean value of the Foz do Iguacu wind velocities in the summer season was used to determine the convection heat transfer coefficient (h).

To determine the effect of temperature on cell efficiency, use Eq. 1 developed by Yamaguchi et al. [72]. Although the mathematical equation of Eq. 1 and Eq. 2 are obtained in a simple way, through temperature tests and verifying the change of efficiency in PV cells in a practical way, the straight-line adjustment method is practical and accurate for these purposes. The results obtained using these equations in research such as: Meral & Dinçer, on the factors that affect the operation and efficiency of photovoltaic cells [73]; Nsengiyumva et. al, on the advances and challenges in solar tracking systems [74]; Silva, on the study and modelling of a photovoltaic solar plant [75]; Bernal, with the development of a photovoltaic cooling system [76];

among others, has been successful in modelling the influence of temperature on photovoltaic cell operation under certain conditions, obtaining accurate results.

$$\eta_{\text{datasheet}} = -0,05 * T_{\text{det}} + X \quad (1)$$

Eq. 1 is specifically developed for a temperature $T_{\text{det}} = T_{\text{det}} = 25^{\circ}\text{C}$ according to STC data and an azimuth angle between 20°C and 25°C according to the geographical specifications of Foz do Iguaçu. The cell efficiency is obtained from datasheet data for STC conditions and the efficiency used is $\eta_{\text{datasheet}} = 16\%$ to a temperature of $T_{\text{det}} = T_{\text{det}} = 25^{\circ}\text{C}$ [72]. Substituting the values of $\eta_{\text{datasheet}}$ and T_{det} in Eq. 1, we determine that the unknown value results in $X = 17,25X = 17,25$. Given the value of X, one can rewrite Eq. 1 to obtain Eq. 2.

$$\eta_{\text{cel}} = -0,05 * T_{\text{cel}} + 17,25 \quad (2)$$

The Eq. 2 is the modified equation of Yamaguchi et al to use the specific efficiency and temperature data from the case study of this research, where T_{cel} is the average temperature reached by the PV arrangement under the simulation conditions and η_{cel} is the resulting efficiency for said temperature.

Conduction heat transfer is modelled by the Fourier conduction law, which in principle assumes that the thermal conductivity of the material (k) is uniform, because the temperature difference between the heat transfer media is very small, and the specific heat at constant pressure (Cp) and specific mass (ρ) are independent of temperature [77]. Subsequently, assuming the assumptions and simulation parameters becomes the equation of Heat Diffusion for Permanent and Generation less Regime described in and Eq. 3 [77].

$$\nabla^2 T = (1/\alpha)(\partial T/\partial t) \quad (3)$$

How TSF and PV system behaviour are measured on STC. The specific mass of the surrounding air was determined as a function of these same characteristics by the ideal gas ratio, resulting in $\rho_{\text{air}} = 1,1841 \text{ kg/m}^3 \rho_{\text{ar}} = 1,1841 \frac{\text{kg}}{\text{m}^3}$ [78]. The coefficient of heat transfer by convection is determined by Eq. 4 [79], using the wind speed average for the summer season in Foz do Iguaçu which is $2,42 \text{ m/s}$ [71].

$$h = 5,7 + 3,8v = 14,89 \text{ W/m}^2.\text{K} \quad (4)$$

When implementing the study, it was assumed that the entire geometry experiences conduction heat exchange. On the other hand, in convection heat transfer use the wind speed and convection heat transfer coefficient specified in Eq. 4, with free convection and forced convection. In the radiation heat- transfer study, a heat flux of 1000 W/m^2 (STC); it is noteworthy that the radiation study will not consider the emissivity and reflectivity in the irradiation conditions.

Convection and radiation heat transfer act only on the surfaces specified with the blue color in Fig. 5 for the integrated and overlapping models. Thermally insulated surfaces for convection and radiation heat transfer are shown in blue in Fig. 6.

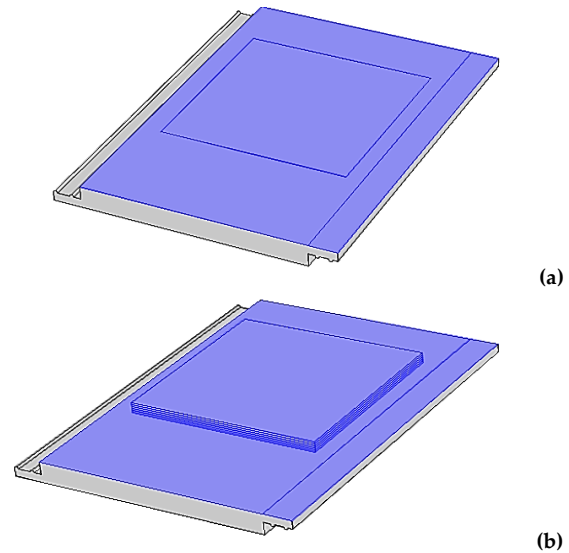


Figure 5. Boundary heat transfer boundary conditions: (a) Integrated model and (b) Superimposed model. Source: The authors.

The blue surfaces of Fig. 6 are isolated from convection heat transfer and radiation flux, as when installing the product on the roof, the blue colored surfaces are arranged on the inner surface of the house, so they are not in contact with the surrounding environment and only exchange heat through the driving mechanism. On the other hand, the grey colored surfaces are in direct contact with the outside at the time of installation, therefore the heat exchange takes place by the three combined mechanisms.

When implementing the simulation, a grid refinement was performed in the PV array, specifying four temperature gradient points for each plate composing the PV array, allowing visualizing the color change and consequently the

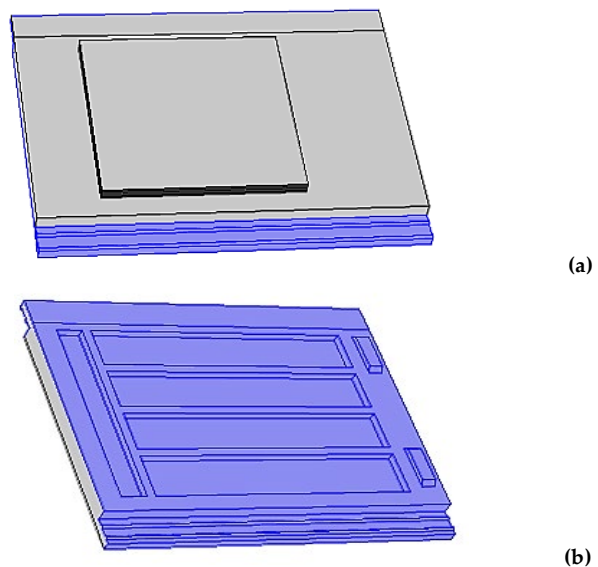


Figure 6. Thermally insulated surfaces for convection and radiation transfer: (a) Top surface view and (b) Bottom surface view. Source: The authors.

temperature variation; similarly, mesh refinement was performed on surfaces exposed to radiation and convection. For the combined study of conduction, convection and radiation was performed the "coupling" of surfaces in both PV and TSF.

3.2 Numerical method

In this section, the results of the temperature distribution on the tiles and the PV arrangement will be presented and discussed. Subsequently, the temperature of the PV cells in the tile is determined to define the efficiency in simulated models using Eq. 2.

Conduction heat-transfer study conditions applied in Comsol Multiphysics® and literature data for convection and radiation for Superimposed (CS) and Integrated (CON) Concrete, Superimposed PV (PS) and Integrated Array Polypropylene (PI), and the overlap model (PVCS) and integrated PVC (PVCI) at the mean maximum temperatures, 30.6 °C and the average minimum temperature of 22.1 °C [71], Fig. 7 and Fig. 8 show the result of the tile temperature distribution and the photovoltaic arrangement for the superimposed and integrated configurations for steady state simulation.

Comparing the results of the overlapping TSF models, it was shown that the upper part of the PV arrangement is the component with the highest radiation exposure corresponding to glass, which has a similar color in the three materials, varying the temperature between 95 °C and 82 °C. On the other hand, comparing the color achieved on the surface exposed to 1000W/m² flow and convection, the model/material that experienced the highest temperature increase is the CS; oppositely, PS had the lowest temperatures on the exposed surface, ranging between 72.23 °C and 80.67 °C.

Comparing the isolated surfaces, PS reaches the lowest temperature in the lower (inner) part of the TSF with temperatures ranging from 72.23 °C to 80.67 °C for studies at 22.1 °C and 30.6 °C respectively.

In the study of the integrated TSF model, it is noticeable the difference of the IC compared to the PI and PVCI, because the concrete tile is strongly affected by temperature, considering its high conductivity (1.80 W/m°C). On the tile surface exposed to 1000 W/m² flow and convection, PI and PVCI act as a thermal insulator, reaching maximum temperatures of 75 °C (test at 30.6 °C) in almost all of the tile geometry.

After the thermal study of the models under conduction heat transfer conditions, the convection and radiation data from the literature, together with the data provided by Eq. 4 and the simulation conditions specified for each mechanism, the temperature of the photovoltaic cell was determined by locating the center point of the structure that represents only the "Solar Cell" layer as shown in Fig. 4 and Table 2 by "N°. 3". This would determine the average temperature at which the cell was subjected under simulated conditions.

With the T_{cel} cell temperature, the cell efficiency for this temperature is determined by means of Eq. 2. The results for each model in the maximum and minimum summer temperature conditions of Foz do Iguaçu and their respective power reduction as a function of efficiency are shown in Table 3.

The Table 3 shows the temperatures found in the cell (T_{cel}) for the maximum and minimum temperature conditions of the external environment (Text), the η_{cel} component is determined using Eq. 2 and substituting T_{cel} for each study, the difference in efficiencies represented by η_{fab} - η_{cel} determined by the subtraction of the efficiency indicated by the manufacturer (η_{fab} = 16%) and the efficiency determined in the study (η_{cel}), which represents the percentage of efficiency decrease under simulated conditions.

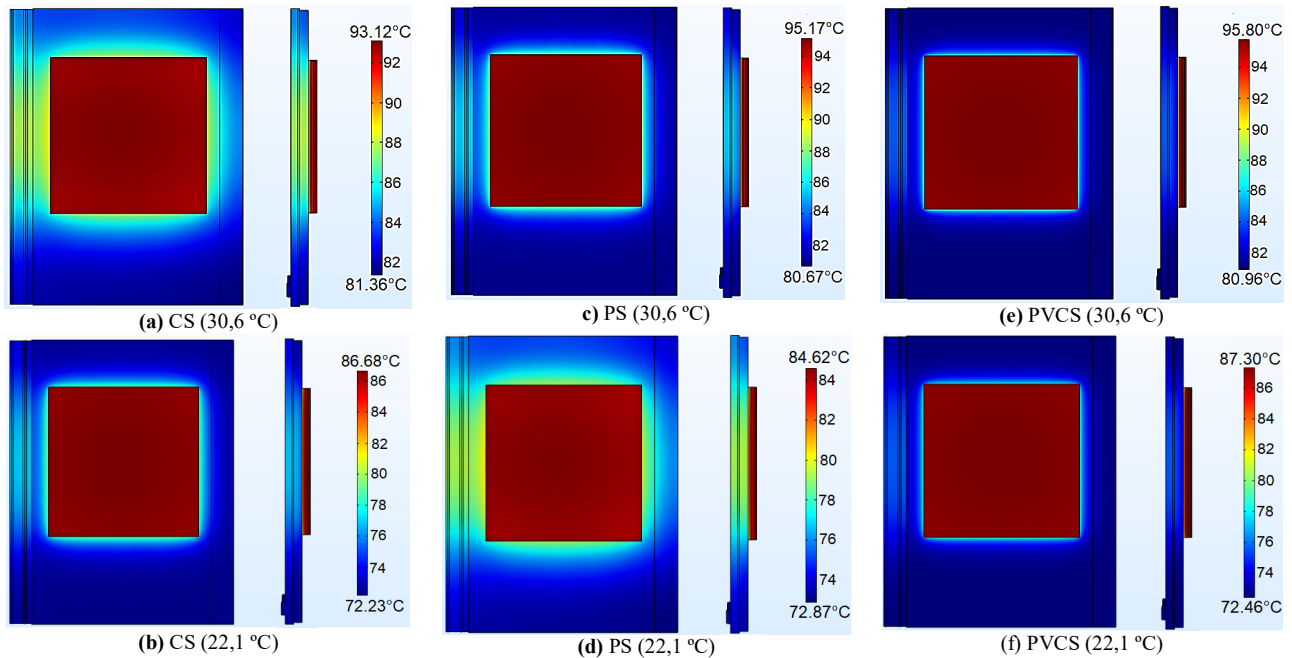


Figure 7. Temperature distribution for overlapping model under maximum and minimum outside temperature conditions for: (a) CS at 30,6°C; (b) CS at 22,1°C; (c) PS at 30,6°C (d) PS at 22,1°C; (e) PVCS at 30,6°C; (f) PVCS at 22,1°C. Source: The authors.

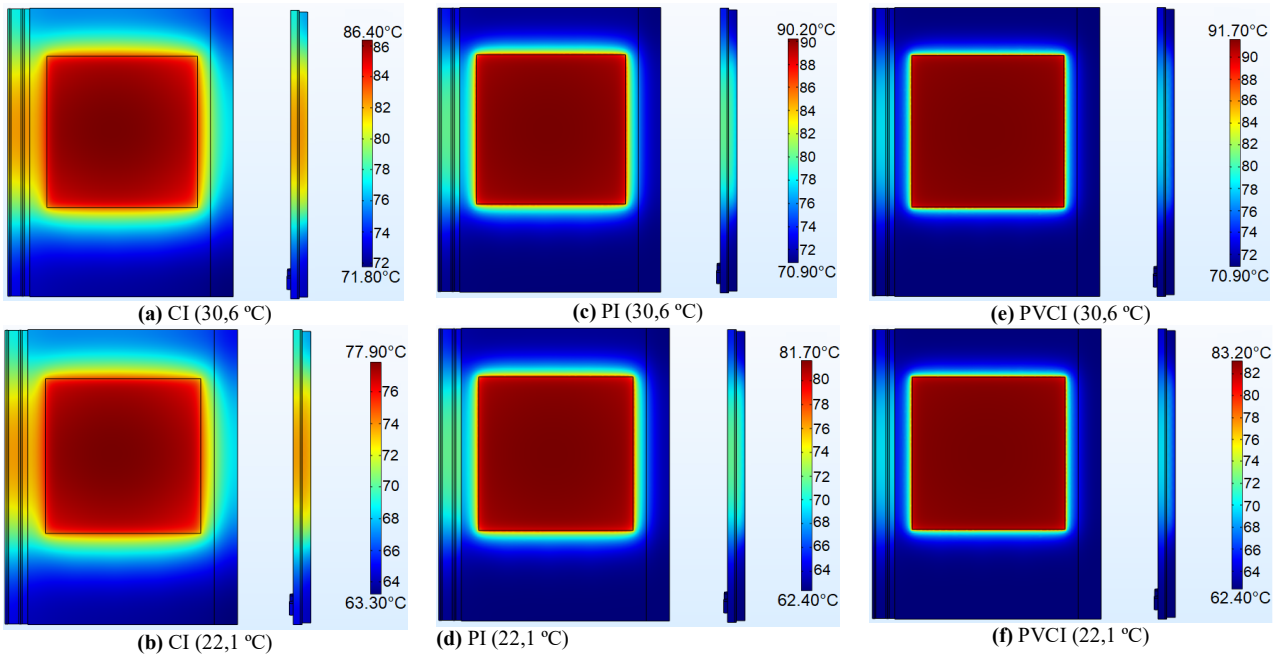


Figure 8. Temperature distribution for integrated model under maximum and minimum outdoor temperature conditions of: (a) CI at 30,6°C; (b) CI at 22,1°C; (c) PI at 30,6°C (d) PI at 22,1°C; (e) PVCI at 30,6°C; (f) PVCI at 22,1°C. Source: The authors.

Table 3. Efficiency of models due to cell temperature for outdoor temperature 30,6 °C and 22.1 °C.

Nº	Model	Text [°C]	Tcel [°C]	η cel [%]	η fab - η cel [%]
1	CS	30,60	92,09	12,65	3,35
2	CI	30,60	85,19	12,99	3,01
3	PS	30,60	94,42	12,53	3,47
4	PI	30,60	89,39	12,78	3,22
5	PVCS	30,60	94,31	12,53	3,47
6	PVCI	30,60	91,10	12,70	3,30
7	CS	22,10	83,61	13,07	2,93
8	CI	22,10	76,64	13,42	2,58
9	PS	22,10	85,91	12,95	3,05
10	PI	22,10	80,73	13,21	2,79
11	PVCS	22,10	86,83	12,91	3,09
12	PVCI	22,10	82,56	13,12	2,88

Source: The authors.

4. Results and discussion

The correlating the results and comparing the proposed models with the materials, the cell temperatures and the determined efficiencies. Subsequently, the results will be approached according to the civil-structural characteristics, characterizing the thermal properties of the tile materials and their influence on the roof structure. Finally, the results obtained will be compared with some conventional photovoltaic systems with different efficiencies, but maintaining the same simulation conditions.

In order to quantify the efficiency performance in simulated models for temperatures between 22.1°C and 30.6°C, Table 4 and Fig. 9 show the temperature interpolations, verifying the change efficiency by increasing the cell temperature by 1°C.

By analyzing the data contained in Table 4 and Fig. 9, it can be shown that the decrease in efficiency occurs linearly by approximately 0.05%/°C for Concrete, Polypropylene and PVC, both in the integrated and overlapping model. Comparing the six test, the IC is the model with the highest performance, with efficiency of 13.42% measured at 22.1°C. On the other hand, when buying the yield on overlapping models, the CS showed the best performance, with an efficiency of 12.93% at 25°C (STC).

When evaluating the materials according to the integrated and overlapping models, it was found that the integrated models showed greater efficiency for the same test conditions; which has a direct relation with the convective effect present in the overlapping models, negatively influencing the cell performance and consequently in the system. The models most affected by the increase in cell temperature in the test condition at 30.6 °C were PS and PVCS, which can be explained by the action of the convective effect of air, with consequently increases the temperature in the cell.

Table 4. Interpolation Of Pv Cell Temperatures For Efficiency For Photovoltaic Arrangement With Overlapping And Integrated Cell.

Tcel [°C]	η CS [%]	η CI [%]	η PS [%]	η PI [%]	η PVCS [%]	η PVCI [%]
22,10	13,07	13,42	12,95	13,21	12,91	13,12
23,00	13,03	13,37	12,91	13,16	12,87	13,08
24,00	12,98	13,32	12,86	13,11	12,83	13,03
25,00	12,93	13,27	12,81	13,06	12,78	12,98
26,00	12,88	13,22	12,76	13,01	12,74	12,93
27,00	12,83	13,17	12,71	12,96	12,69	12,88
28,00	12,78	13,12	12,66	12,91	12,65	12,83
29,00	12,73	13,07	12,61	12,86	12,60	12,78
30,00	12,68	13,02	12,56	12,81	12,56	12,73
30,60	12,65	12,99	12,53	12,78	12,53	12,70

Source: The authors.

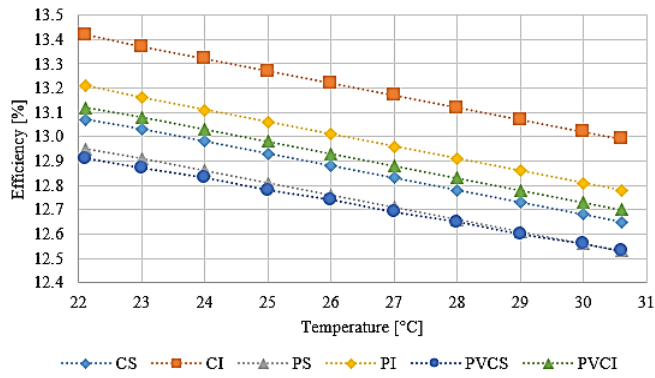


Figure 9. PV cell temperature interpolation as a function of efficiency for overlay and integrated models. Source: The authors.

Due to the very characteristic of BIPV and specifically the solar tiles evaluated in the research, it is interesting to analyse the materials comparatively from the standpoint of efficiency individually. It also characterizes the civil-structural advantages that these materials can bring to the structure, since the use of a certain material in the roof structure brings individual and specific characteristics that will be decisive when specifying the installation location. Some of the features are thermal comfort, hardness of the roof, less weight to the structure, environmentally friendly, etc.

By implementing mesh refinement for four gradient points on each plate, it is possible to see the temperature gradient in the PV arrangement represented by the color change in the results of Fig. 7 and Fig. 8, which varies up to 10°C when compared in simulated studies at 22.1°C and 30.6°C, reflecting the importance of a correct simulation.

4.1 Civil-structural

From a civil-structural point of view, TSF materials have several characteristics that influence the structure, for example, the high specific mass polypropylene (910 kg/m³) has advantage in lower weight to the structure [83], however, it has lower hardness with a value of 67-74 Shore D [84], when compared to the hardness of the PVC of 80-83 Shore D [84]; Shore D hardness for concrete has no measurable value as it is a completely rigid material. While thermally polypropylene acts as an insulator between the external and

internal environment by the low thermal conductivity value of 0,25 W/m°C, also has a melting temperature above 140°C and glass transition temperature between -30°C and 0°C, therefore there is no risk of melting or “freezing” of the material operating under normal operating conditions, so this material is recommended for climates where the temperature does not drop below 0 °C or with hail that could damage the structure [85,86].

On the other hand, concrete has high compressive strength (approx. 23 MPa) [87] and low flexural strength (approx. 2.4 MPa) [88], what makes from great material external impact resistor [89]. It is also noted that it has the advantage of being waterproof or permeable depending on the case, preventing the entry of water or absorbing it to cool the material and consequently the arrangement PV cells [88]. However, the high weight of the structure and the heat absorbing the impermeable concrete can overheat the internal environment of the structure, so it is advisable to avoid concrete tiles in high temperature places [90].

While PVC has among its advantages being a material that can be reused 100% because it is recyclable [91]. As Polypropylene, or PVC stands out for being a lightweight product matching the specific masses of 910 kg/m³ for Polypropylene and 1760 kg/m³ for PVC, without a sturdy base, which speeds up the construction process and lowers investment costs without a sturdy base, which speeds up the construction process and lowers investment costs [92]. As for thermal comfort is an insulating material with a value of 0.10 W/m°C, reducing the effect of thermal exchange with the external environment. Conventional System Comparison

By comparing the effect of decreasing temperature efficiency for conventional PV systems and the studied TSF, the data collected in Table 5 and visualized in Fig. 10 for different technologies are displayed. The comparison is made under irradiation conditions of 1000 W/m² for conventional polycrystalline (PC), monocrystalline (MC) and CIS photovoltaic technologies.

As the data in Table 5 and Fig. 10 show, depending on the PV technology and the presence of silicon as the base material in the composition of the modules, the behavior of efficiency as a function of temperature increase experiences considerable changes. Similarly in the case with CIS cells, which use Copper and Indium Diselenium (CuInSe₂) as active semiconductor material in cells rather than Silicon in large percentage [93].

Table 5. Interpolation Of Temperatures According To Reducing Electrical Efficiency For Different Photovoltaic Technologies.

T cel [°C]	η CS [%]	η CI [%]	η PS [%]	η PI [%]	η PVCS [%]	η PVCI [%]	η PC [%]	η MC [%]	η CIS [%]
5,5	13,0	13,4	12,9	13,2	12,9	13,1	11,7	14,9	11,9
23,0	13,0	13,4	12,9	13,1	12,8	13,0	11,6	14,9	11,8
24,0	12,9	13,3	12,8	13,1	12,8	13,0	11,6	14,8	11,5
25,0	12,9	13,3	12,8	13,0	12,7	12,9	11,5	14,7	11,3
26,0	12,9	13,2	12,7	13,0	12,7	12,9	11,5	14,7	11,1
27,0	12,8	13,2	12,7	12,9	12,6	12,8	11,4	14,6	11,0
28,0	12,8	13,1	12,6	12,9	12,6	12,8	11,4	14,5	10,8
29,0	12,7	13,1	12,6	12,8	12,6	12,7	11,3	14,5	10,5
30,0	12,7	13,0	12,5	12,8	12,5	12,7	11,3	14,4	10,2
30,6	12,6	12,9	12,5	12,7	12,5	12,7	11,2	14,3	9,8

Source: Adapted from Gedik, 2016; Ray, 2010 and Fesharaki et al., 2011.

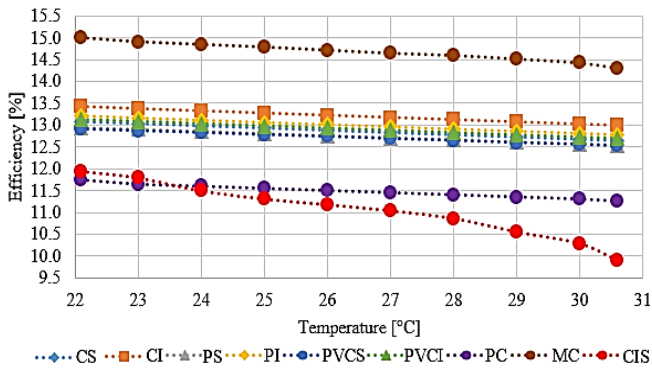


Figure 10. Comparison of cell temperatures as a function of efficiency for different photovoltaic technologies.

Source: Adapted from Gedik, 2016; Ray, 2010 and Fesharaki et al., 2011.

In the studies of the evaluated TSF and the CP, the decrease of the efficiency happens value of $0,05\%/^{\circ}\text{C}$ [94], on the other hand for MC and CIS technology, the decrease occurs in the order of $0,09\%/^{\circ}\text{C}$ and $0,24\%/^{\circ}\text{C}$ respectively, reflecting an important difference in behaviors.

As shown in the comparative study of PV technologies, the cells with the highest yield are cells with the presence of silicon as a major component, in this sense when there is more space available for the installation of TSF, these technologies will have the advantage of higher throughput per square meter. However, thin-film cells, as in the case of CIS, will need less input of material and energy to make the PV array, a factor that will be reflected in the final price of these cells [93].

5. Conclusions

The Building Integrated Photovoltaics (BIPVs) technologies have a promising outlook in the near future. As the cost of manufacturing is expected to decrease, it will increase competitiveness and consequently add new TSF models and manufacturers, thus making this technology extremely competitive with conventional PV systems applied to building systems.

However, in order to properly assert its use, market insertion and competitiveness with conventional PV systems, there is a need, as evidenced in the research, to take into account several factors such as: (i) the materials as a function of the thermal properties that they can provide both in PV arrangement influencing the temperature of cells, cooling the PV system, providing characteristics of thermal comfort, among others; (ii) civil and structural advantages such as lower weight, greater roof resistance to impacts and extreme climates; (iii) characteristics of the installation site, factor directly related to temperature, wind speed, relative humidity and irradiation; (iv) lowering the cost of integrated building technology by combining factors/advantages beyond the power supply function.

Hopefully, in the coming decades, conventional and unconventional photovoltaic technologies can make a substantial contribution to global and centralized energy production, although currently its cost is up to five times more expensive than conventional power grid due to low

production costs from non-renewable sources.

According to the analysis of the simulations performed in the integrated and superimposed PV arrangement models, for Concrete, Polypropylene and PVC materials, by means of simulated conduction heat transfer in the Comsol Multiphysics® software, data from convection and radiation literature, shown in Fig. 7 and Fig. 8, to determine the influence of cell operating temperature by means of the efficiency calculation using Eq. 2, and the results shown in Table 3 and Table 4, it was proved that the integrated and overlapping models for the Concrete, Polypropylene and PVC have clearly differentiated cell performances, with efficiency variations between 12.53% and 13.42% for the analyzed models.

Thermally, the simulated PVC and Polypropylene models, comparing the superimposed and integrated PV array configurations, experienced similar results in the temperature reached in the tiles, with a difference of approximately 3°C more for polypropylene, which is reasonable for the higher material thermal conductivity value. On the other hand, the concrete presented different values to PVC and Polypropylene, reaching the highest temperatures in the tile geometry.

Considering that the use of TSF using as concrete base material Concrete, Polypropylene and PVC with the thermal characteristics mentioned in Table 2 has different behaviors, it is essential to verify the contribution of the civil and structural characteristics that support these products.

As found in the study, the variation in efficiency for all models and materials studied presented in, happens in $0,05\%/^{\circ}\text{C}$. Although this value is considered as minimal and negligible, it is essential to verify how economically this data represents in the TSF, because in terms of comparing annual consumption and savings against the efficiency of a given model and material with a conventional PV system, it could mean real savings in consumption, and consider the civil and structural advantages that the materials bring.

Therefore, according to the analysis of the results obtained in this research it can be stated that: For the Concrete, Polypropylene and PVC studied, both for the integrated and superimposed PV arrangement model for the TSF, when simulating the product in STC, the efficiency decrease with the temperature increase happens in a value of $0,05\%/^{\circ}\text{C}$. The diminishing effect of $0,05\%/^{\circ}\text{C}$ happens for the thermal properties of the tile materials with varying thermal conductivity of the tile materials. $0,1\text{W}/\text{m}^{\circ}\text{C}$ to $1,80\text{W}/\text{m}^{\circ}\text{C}$, specific heat the constant pressure of $850\text{J}/\text{kg}^{\circ}\text{C}$ to $1700\text{J}/\text{kg}^{\circ}\text{C}$ and specific mass between $910\text{ kg}/\text{m}^3$ to $2300\text{ kg}/\text{m}^3$. Therefore, for TSF studies under STC conditions for the characteristics of Foz do Iguaçu and varying the thermal conditions of thermal conductivity, specific heat at constant pressure and specific mass of any tile material, within the range of the specified values and maintaining the PV array characteristics resulted in efficiency behaviors between the 12,53% to 13,42%.

Bearing in mind that the effect of decreasing efficiency on $0,05\%/^{\circ}\text{C}$ Both in the integrated and overlapping models for Concrete, Polypropylene and PVC happens differently. These proves that it is relevant to check the input of materials from civil and structural perspective that they can bring to the

roof, as the same simulated materials -but with different models- show different TSF thermal behaviors in relation to the temperature reached by the tile. In the simulated CS and IC the 30,6°C, the minimum temperature reached by the tile is 81,36°C and 71,80°C respectively, which evidences that the CS model brought a higher temperature to the internal environment of the house, directly influenced on the thermal comfort.

The same effect happens with the study of simulated PS and IP at 30.6°C, where the minimum temperature reached is 80,67°C and 70,90°C respectively; therefore, the PI will point out the best thermal comfort features that the PS. As in previous cases, PPCI has better thermal comfort characteristics when compacted with PVCS as it has temperature differences of up to 10°C when analyzing the same point of geometry.

Finally, as a continuation of this research, it is suggested to broaden the scope of the simulation including new materials, different geometric shapes of tiles, irradiation conditions and economic factors that influence the commercialization and replacement of the conventional photovoltaic technology for the BIPV's range.

In addition, has the development of hybrid generation systems for harnessing thermal energy based in energy harvesting [95-99].

Acknowledgment

This research was funded by Federal University of Latin American Integration (UNILA), supported by 'Triple Agenda' Institutional Program (Agenda Tríplice). The O.H.A.J. was funded by the Brazilian National Council for Scientific and Technological Development (CNPq), grant number 307223/2017-5 and 407531/2018-1.

References

- [1] REN21, Renewables 2017: Global Status Report. Renewable Energy Policy Network for the 21st Century, 2017.
- [2] Marcovitch, J., A redução de emissões de gases de efeito estufa e a legislação brasileira, FEA/USP.
- [3] BRASIL, Lei N° 10.438. Brasil, 2010, pp. 2100-2125.
- [4] Marcovitch, J., Para mudar o futuro: mudanças climáticas, políticas públicas e estratégias empresariais, 1^{ra} ed.. São Paulo, Brasil, 2006.
- [5] Energia, F., Uma análise comparativa da transição energética na América Latina e Europa, FGV Energia, 2016.
- [6] Bueno, E., Atlas Brasileiro de Energia Solar, 2^{da} Ed.. São José dos Campos, Brasil, 2017.
- [7] De Nys, E., Engle, N.L. and Magalhães, A.R., Secas no Brasil: políticas e gestão proativas, 2016.
- [8] Martins, E.S.P.R., De Nys, E., Molejón, C., Biazeto, B., Silva, R.F.V. and Engle, N., Série água Brasil: monitor de secas do nordeste, em busca de um novo paradigma para a gestão de secas(January), Banco Mundial, Brasília, DF, Brasil, 2015.
- [9] ANEEL, Atlas de Energia Elétrica do Brasil, 1^{ra} Ed., 2002.
- [10] Rastogi, S., Singh, A. and Upadhyay, M.P., Study of different issues and challenges of wind energy generation, Int. J. Adv. Res. Sci. Eng., 5, pp. 380-384, 2016.
- [11] Benemann, J., Chehab, O. and Schaar-Gabriel, E., Building-integrated PV modules, Sol. Energy Mater. Sol. Cells, 67(1-4), pp. 345-354, 2001. DOI:10.1016/S0927-0248(00)00302-0.
- [12] Rütter, R., Edifícios solares fotovoltaicos: o potencial da geração solar fotovoltaica integrada a edificações urbanas e interligada à rede elétrica pública no Brasil, 2004.
- [13] Radziemska, E., The effect of temperature on the power drop in crystalline silicon solar cells, Renew. Energy, 28, pp. 1-12, 2003. DOI: 10.1016/S0960-1481(02)00015-0.
- [14] Barçante, T., Influência da temperatura em aglomerados auto-reconfiguráveis de células solares fotovoltaicas, Tesis de Grado, Universidade Federal de Minas Gerais, Brasil, 2008.
- [15] Al-naser, Q.A.H., Al-barghoothi, N.M.A. and Al-ali, N.A.S., The effect of temperature variations on solar cell efficiency, Int. J. Eng., Bus. Enterp. Appl., pp. 108-112, 2013.
- [16] Green, M., Third generation photovoltaics: advanced solar energy conversion, 1^{ra} ed. Springer, Sydney, Australia, 2003.
- [17] Boreland, M. and Bagnall, D., Current and future photovoltaics, commissioned report for office of science and innovation - Foresight and horizon scanning centre - Energy Project, 2015, pp. 1-17.
- [18] Fthenakis, V., Third generation photovoltaics, 1^{ra} ed. InTech, Rijeka, Croatia, 2012.
- [19] Ely, F. and Swart, J., Energia solar fotovoltaica de terceira geração, IEEE, 2014, pp. 138-139,
- [20] Conibeer, G., Third-generation photovoltaics, Materials Today, 10, pp. 42-50, 2007. DOI:10.1016/S1369-7021(07)70278-x.
- [21] Spanggaard, H. and Krebs, F.C., A brief history of the development of organic and polymeric photovoltaics, Sol. Energy Mater. Sol. Cells, 83(2-3), pp. 125-146, 2004. DOI:10.1016/j.solmat.2004.02.021
- [22] Shukla, A.K. Sudhakar, K. Baredar, P. and Mamat, R., Solar PV and BIPV system: barrier, challenges and policy recommendations in India, Renew. Sustain. Energy Rev., 82(October), pp. 3314-3322, 2018. DOI:10.1016/j.rser.2017.10.013.
- [23] Shukla, A.K. Sudhakar, K. and Baredar, P., Recent advancement in BIPV product technologies: a review, Energy Build., 140, pp. 188-195, 2017. DOI: 10.1016/j.enbuild.2017.02.015.
- [24] Guerrero-Gutiérrez, E., Communication from the commission to the European Parliament, the council, the European Economic and Social Committee and the Committee of the Regions, Europe 2020 Flagship Initiative, Brussels, Belgium, 2010.
- [25] Debbarma, M., Sudhakar, and Baredar, P., Comparison of BIPV and BIPVT: a review, Resour. Technol., 3, pp. 263-271, 2016. DOI: 10.1016/j.refit.2016.11.013.
- [26] Shukla, K.N. Rangnekar, S. and Sudhakar, K., Mathematical modelling of solar radiation incident on tilted surface for photovoltaic application at Bhopal, M.P., India, Int. J. Ambient Energy, 37(6), pp. 579-588, 2016. DOI: 10.1080/01430750.2015.1023834
- [27] Hammond, G.P. Harajli, H.A. Jones, C.I. and Winnett, A.B., Whole systems appraisal of a UK Building Integrated Photovoltaic (BIPV) system: energy, environmental, and economic evaluations, Energy Policy, 40, pp. 219-230, 2012. DOI: 10.1016/j.enpol.2011.09.048.
- [28] Peng, J. Lu, L. and Yang, H., Review on life cycle assessment of energy payback and greenhouse gas emission of solar photovoltaic systems, Renew. Sustain. Energy Rev., 19, pp. 255-274, 2013. DOI: 10.1016/j.rser.2012.11.035.
- [29] Peng, C. Huang, Y. and Wu, Z., Building-integrated photovoltaics (BIPV) in architectural design in China, Energy Build., 43(12), pp. 3592-3598, 2011. DOI: 10.1016/j.enbuild.2011.09.032
- [30] Bloem, J.J. Lodi, C., Cipriano, J. and Chemisana, D., An outdoor Test reference environment for double skin applications of Building integrated photovoltaic systems, Energy Build., 50, pp. 63-73, 2012. DOI: 10.1016/j.enbuild.2012.03.023.
- [31] Oliver, M. and Jackson, T., Energy and economic evaluation of building-integrated photovoltaics, Pergamon, 26, pp. 431-439, 2001. DOI: 10.1016/S0360-5442(01)00009-3.
- [32] Shukla, K.N. Rangnekar, S. and Sudhakar, K., Comparative study of isotropic and anisotropic sky models to estimate solar radiation incident on tilted surface: a case study for Bhopal, India, Energy Reports, 1, pp. 96-103, 2015. DOI: 10.1016/j.egy.2015.03.003.
- [33] Shukla, A.K. Sudhakar, K. and Baredar, P., Simulation and performance analysis of 110 kW p grid-connected photovoltaic system for residential building in India: a comparative analysis of various PV technology, Energy Reports, 2, pp. 82-88, 2016. DOI: 10.1016/j.egy.2016.04.001.
- [34] Biyik, E. et al., A key review of building integrated photovoltaic (BIPV) systems, Eng. Sci. Technol. an Int. J., 20(3), pp. 833-858, 2017. DOI: 10.1016/j.jestech.2017.01.009.

- [35] Oliver, M. and Jackson, T., The evolution of economic and environmental cost for crystalline silicon photovoltaics, *Energy Policy*, 28, pp. 1011-1021, 2000. DOI: 10.1016/S0301-4215(00)0088-4.
- [36] Herig, C., Using photovoltaics to preserve California's electricity capacity reserves. National Renewable Energy Laboratory, 2001.
- [37] Zilli, B.M. et al., Performance and effect of water-cooling on a microgeneration system of photovoltaic solar energy in Paraná, Brazil, *Clean. Prod.*, 192, pp. 477-485, 2018. DOI: 10.1016/j.jclepro.2018.04.241.
- [38] Cronemberger, J., Integración de sistemas fotovoltaicos en edificios de oficinas en bajas latitudes: estudio del balance energético aplicado a Brasil, Tesis, Universidad Politécnica de Madrid, 2015.
- [39] Yang, H., Burnett, J. and Ji, J., Simple approach to cooling load component calculation through PV walls, *Energy Build.*, 31, pp. 285-290, 2000. DOI: 10.1016/S0378-7788(99)00041-9.
- [40] Sandberg M. and Moshfegh, B., Investigation of fluid flow and heat transfer in a vertical channel heat from one side by PV elements, *Spec. Issue World Renew. Energy Congr.*, 8, pp. 254-258, 1996. DOI: 10.1016/0960-1481(96)88857-4.
- [41] Krauter, S., Araujo, R.G. Schroer, S., Hanitsch, R., Salhi, M.J. and Triebel, C., Combined photovoltaic and solar thermal systems for facade integration and building insulation, *Sol. Energy*, 67, pp. 239-248, 2000. DOI: 10.1016/S0038-092X(00)00071-2
- [42] Gutschker, O. and Rogass, H., Simulation of a photovoltaic hybrid facade, in: *International Building Performance Simulation Association*, 1997.
- [43] Infield, D., Eicker, U., Fux, V. and Mei, L., A simplified approach to thermal performance calculation for building integrated mechanically ventilated PV facades, *Build. Environ.*, 41, pp. 893-901, 2006. DOI: 10.1016/j.buildenv.2005.04.010.
- [44] Eicker, U., Fux, V., Bauer, U., Mei, L. and Infield, D., Facades and summer performance of buildings, *Energy Build.*, 40, pp. 600-611, 2008. DOI: 10.1016/j.enbuild.2007.04.018.
- [45] Lodi, C., Bacher, P., Cipriano, J. and Madsen, H., Modelling the heat dynamics of a monitored Test Reference Environment for Building Integrated Photovoltaic systems using stochastic differential equations, *Energy Build.*, 50, pp. 273-281, 2012. DOI: 10.1016/j.enbuild.2012.03.046.
- [46] Ng, P., Mithraratne, N. and Wei, H., Energy analysis of semi-transparent BIPV in Singapore buildings, *Energy Build.*, 66, pp. 274-281, 2013. DOI: 10.1016/j.enbuild.2013.07.029.
- [47] Khai, P. and Mithraratne, N., Lifetime performance of semi-transparent building-integrated photovoltaic (BIPV) glazing systems in the tropics, *Renew. Sustain. Energy Rev.*, 31, pp. 736-745, 2014. DOI: 10.1016/j.rser.2013.12.044.
- [48] Huang, M.J. Eames, P.C. and Norton, B., Thermal regulation of building-integrated photovoltaics using phase change materials, *Int. J. Heat Mass Transf.*, 47, pp. 2715-2733, 2004. DOI: 10.1016/j.ijheatmasstransfer.2003.11.015.
- [49] Ma, T., Yang, H., Zhang, Y., Lu, L. and Wang, X., Using phase change materials in photovoltaic systems for thermal regulation and electrical efficiency improvement: a review and outlook, *Renew. Sustain. Energy Rev.*, 43, pp. 1273-1284, 2015. DOI: 10.1016/j.rser.2014.12.003.
- [50] Browne, M.C. Norton, B. and McCormack, S.J., Phase change materials for photovoltaic thermal management, *Renew. Sustain. Energy Rev.*, 47, pp. 762-782, 2015. DOI: 10.1016/j.rser.2015.03.050.
- [51] Rütther, R., The first grid-connected, building-integrated, thin film solar photovoltaic installation in Brazil. 1996.
- [52] Zilles, R. and Oliveira, S., 6.3kWp photovoltaic building integration at São Paulo University, in 17th European Photovoltaic Solar Energy Conference, 2001.
- [53] Inaugurada a primeira central fotovoltaica num estadio do Mundial de Brasil, *PV Magazine: Photovoltaic, Market & Technologie*, May-2013.
- [54] Van del Linden, T. and Szabolcs, M., Los estadios más solares del mundo, *Suplemento Energías renovables*, pp. 42-48, 2018.
- [55] A energia solar nos estádios de futebol do Brasil, *Green Bras: energia limpa para todos*, 2015.
- [56] Ladrilhos metálicos que geram eletricidade, *Csem Brasil*, 2018.
- [57] ECOsolarroof, Solar roof tile, 2017.
- [58] N330 (VBHN330SJ47), solar panel Panasonic Electric Works Europe AG, 2018.
- [59] Marafião, F.P. Alonso, A.M.D.S., Gonçalves, F.A.S. Brandão, D.I., Martins, A.C. G. and Morales-Paredes, H.K., Trends and constraints on Brazilian photovoltaic industry: energy policies, interconnection codes and equipment certification, *IEEE Trans. Ind. Appl.*, 54(5), pp. 4017-4027, 2018. DOI: 10.1109/TIA.2018.2833422
- [60] Omer, S.A. Wilson, R. and Riffat, S.B., Monitoring results of two examples of building integrated PV (BIPV) systems in the UK, *Renew. Energy*, 28, pp. 1387-1399, 2003. DOI: 10.1016/S0960-1481(02)00257-4.
- [61] Agrawal, B. and Tiwari, G., An energy and exergy analysis of building integrated photovoltaic thermal systems, *Energy Sources, Part A Recover. Util. Environ. Eff.*, 33, pp. 649-664, 2010. DOI: 10.1080/15567030903226280.
- [62] Chen, Y., Athienitis, A.K. and Galal, K., Modeling, design and thermal performance of a BIPV / T system thermally coupled with a ventilated concrete slab in a low energy solar house: Part 1, BIPV / T system and house energy concept, *Sol. Energy*, 84(11), pp. 1892-1907, 2010. DOI: 10.1016/j.solener.2010.06.013.
- [63] Chen, Y., Galal, K. and Athienitis, A.K., Modeling, design and thermal performance of a BIPV / T system thermally coupled with a ventilated concrete slab in a low energy solar house: Part 2, ventilated concrete slab, *Sol. Energy*, 84(11), pp. 1908-1919, 2010. DOI: 10.1016/j.solener.2010.06.013.
- [64] Essah, E., Rodriguez, A. and Glover, N., Assessing the performance of a building integrated BP c-Si PV system, *Renew. Energy*, pp. 1-10, 2014. DOI: 10.1016/j.renene.2014.04.002.
- [65] Portolan, Í. and Rütther, R., The potential of building-integrated (BIPV) and building-applied photovoltaics (BAPV) in single-family, urban residences at low latitudes in Brazil, *Energy Build.*, 50, pp. 290-297, 2012. DOI: 10.1016/j.enbuild.2012.03.052.
- [66] Vats, K. and Tiwari, G.N., Performance evaluation of a building integrated semitransparent photovoltaic thermal system for roof and facade, *Energy Build.*, 45, pp. 211-218, 2012. DOI: 10.1016/j.enbuild.2011.11.008.
- [67] Comsol Multiphysics®. 2014.
- [68] Leow, W.Z. et al., Investigation of solar panel performance based on different wind velocity using ANSYS, *Indones. J. Electr. Eng. Comput. Sci.*, 1(3), pp. 456-463, 2016.
- [69] BRASKEM, Propriedades de referência dos compostos de PVC. Boletim Técnico N° 3 PVC, BRASKEM, 2012.
- [70] IMCPLAS, Polipropileno (PP), IMCPLAS, 2018.
- [71] INMET, Consulta dados da estação automática: Foz do Iguaçu (PR), 21/12/2017 a 20/03/2018, Instituto Nacional de Meteorologia, 2018.
- [72] Yamaguchi, T. et al., Data analysis on performance of Pv system installed in south north directions, in: 3rd World Conference on Photovoltaic Energy Conversion, 2003, pp. 2239-2242.
- [73] Meral, M.E. and Dinçer, F., A review of the factors affecting operation and efficiency of photovoltaic based electricity generation systems, *Renew. Sustain. Energy Rev.*, 15(5), pp. 2176-2184, 2011. DOI: 10.1016/j.rser.2011.01.010.
- [74] Nsengiyumva, W., Chen, S.G. Hu, L. and Chen, X., Recent advancements and challenges in Solar Tracking Systems (STS): a review, Elsevier Ltd, 2018. DOI: 10.1016/j.rser.2017.06.085.
- [75] Da Silva, V.O., Estudo e modelagem da arquitetura modular de uma usina solar fotovoltaica arrefecida com protótipo de verificação, Escola Politécnica da Universidade de São Paulo, Brasil, 2015.
- [76] Bernal, J.L. et al., Experimental development of cooling system addressing to photovoltaic power plant in real scale, *Espacios*, 39(4), art. 33, 2018.
- [77] Çengel, Y. and Ghajar, A., *Transferência de Calor e Massa: uma abordagem prática*, 4^{ta} ed. MC Grau Hill, 2012.
- [78] Çengel, Y., Cimbala, J., Saltara, F., Burr, K. and Baliño, J.K., *Mecânica de fluidos: fundamentos y aplicaciones*, 3^{ra} Ed. Mc Graw Hill, 2015.
- [79] Razak, A., Irwan, Y., Leow, W.Z. Irwanto, M., Safwati, I. and Zhafarina, M., Investigation of the effect temperature on photovoltaic (PV) panel output performance, *Int. J. Adv. Sci. Eng. Inf. Technol.*, 6(5), art. 682, 2016.

- [80] Gedik, E., Experimental investigation of module temperature effect on photovoltaic panels efficiency, *J. Polytech.*, 19(194), pp. 569-576, 2016.
- [81] Ray, K.L., Photovoltaic cell efficiency at elevated temperatures by photovoltaic cell efficiency at elevated temperatures, Thesis (S.B.), Dept. of Mechanical Engineering, Massachusetts Institute of Technology MIT, Cambridge, USA, 2010, 23 P.
- [82] Fesharaki, V.J. Dehghani, M. Fesharaki, J.J. and Tavasoli, H., The effect of temperature on photovoltaic cell efficiency, *Emerg. Trends Energy Conserv. ETEC(November)*, pp. 20-21, 2011.
- [83] Salvador, M.M., Amigo, V., Nuez, A., Sahuquillo, O. y Llorens, R., Caracterización de fibras vegetales utilizadas como refuerzo en matrices termoplásticas, *AIMPLAS*, 2008, 4 P.
- [84] VampTech, Polipropileno, VampTech-Ibérica, 2018.
- [85] Caicedo, Á.N., Crespo, C. y De La Cruz, L., Propiedades termomecánicas del Polipropileno: efectos durante el reprocesamiento, *Ing. Investig. y Tecnol.*, XVIII(3), pp. 245-252, 2017.
- [86] Essentia, información sobre el polipropileno y generalidades. 2017.
- [87] NRMCA, CIP 35 - Prueba de resistencia a la compresión del concreto, el concreto en la práctica ¿Qué, por qué y cómo?, 2019.
- [88] Concreto permeable: alternativas sustentables, *Construcción y Tecnología en Concreto*, 2018.
- [89] Pinheiro, L.M. Muzardo, C.D. and Santos, S.P., Cap. 2: características do concreto, in *estruturas de concreto*, USP and EESC, Eds. 2004, pp. 2.1-2.10.
- [90] EMONO, Vantagens e desvantagens da telha de concreto, *EMONO*, 2019.
- [91] Pita, V.J.R.R., Sampaio, E.E.M. and Monteiro, C.E.E., Mechanical properties evaluation of PVC / plasticizers and PVC / thermoplastic polyurethane blends from extrusion processing, *Polym. Test.*, 21, pp. 545-550, 2002. DOI: 10.1016/S0142-9418(01)00122-2
- [92] Canevarolo, S., *Ciência dos polímeros: um texto básico para tecnólogos e engenheiros*, 2^{da} ed., 2006.
- [93] Influencia de la tecnología fotovoltaica en la producción energética, células fotovoltaicas, Sevilla, España, 2018.
- [94] Bloem, J.J., Evaluation of a PV-integrated building application in a well-controlled outdoor test environment, *Building Environment*, 43, pp. 205-216, 2008. DOI: 10.1016/j.buildenv.2006.10.041.
- [95] Calderón-Henao, N., Venturini, O.J., Franco, E.H.M., Silva-Lora, E., Scherer, H.F., Maya, D.M.Y. and Ando Junior, O.H., Numerical-experimental performance assessment of a non-concentrating Solar Thermoelectric Generator (STEG) Operating in the Southern Hemisphere. *Energies*, 13, art. 2666. 2020. DOI: 10.3390/en13102666
- [96] Izidoro, C.L., Ando Junior, O.H., Carmo, J.P. and Schaeffer, L., Characterization of thermoelectric generator for energy harvesting, *Measurement*, 106, pp. 283-290, 2017. DOI: 10.1016/j.measurement.2016.01.010.
- [97] Ando Junior, O.H., Calderon, N.H. and De Souza, S.S., Characterization of a Thermoelectric Generator (TEG) system for waste heat recovery. *Energies*, 11, art. 1555, 2018. DOI: 10.3390/en11061555
- [98] Kramer, L.R., Maran, A.L.O., de Souza, S.S. and Ando Junior, O.H., Analytical and numerical study for the determination of a thermoelectric generator's internal resistance. *Energies*, 12, art. 3053. 2019. DOI: 10.3390/en12163053
- [99] Maran, A.L.O., Henao, N.C., Silva, E.A., Schaeffer, L. and Ando Junior, O.H., Use of the Seebeck effect for energy harvesting, *IEEE Latin America Transactions*, 14(9), pp. 4106-4114, 2016, DOI: 10.1109/TLA.2016.7785940.
- C. Becerra-Díaz**, is BSc. Eng. in Energy Engineer from the Federal University of Latin American Integration, UNILA, Brazil. It has in the areas of synthesis of electrocatalysts, modeling of thermal systems and electrical systems, acting in the areas: characterization of graphene and graphene oxide, cooling of nickel-sodium experiment cells and modeling of thermoelectric power plants.
ORCID: 0000-0003-2746-6321
- O.H Ando Junior**, is BSc. Eng. in Electrical Engineering and Sp. in Business Management from Universidade Luterana do Brasil, ULBRA, Brazil, with a MSc. and PhD in Engineering from Universidad Federal de Rio Grande del Sur, UFRGS, Brazil. Professor at UNILA, He is currently an ad hoc consultant for CNPq, reviewer of several Journals and Associate Editor of IEEE Latin American Transactions. Acting in the areas: energy capture, energy conversion, electric power quality and power systems.
ORCID: 0000-0002-6951-0063